

Contribution from the Laboratorium für Anorganische Chemie, ETH-Zentrum, CH-8092 Zürich, Switzerland, and Forschungsdienste Physik, Ciba Geigy AG, CH-4002 Basel, Switzerland

Electrochemical Reduction of Complexes Containing the $[\text{Mo}_3\text{S}(\text{S}_2)_3]^{4+}$ Core in Aqueous Media and the Structure of Bis(triethylammonium) Tris(2-mercaptobenzoato)tris(μ -disulfido)(μ_3 -thio)-triangulo-trimolybdate(IV)

Kaspar Hegetschweiler,^{*1a} Thomas Keller,^{1a} Martin Bäumle,^{1a} Greti Rihs,^{1b} and Walter Schneider^{1a}

Received April 23, 1991

The electrochemical reduction of complexes containing the $\text{Mo}_3\text{S}(\text{S}_2)_3$ core with 2-mercaptosuccinic acid (H_3msa), 2,3-dimercaptosuccinic acid (H_4dsa), 3,4-dihydroxybenzoic acid (H_3dba), and 2-mercaptobenzoic acid (H_2mba) was investigated by polarography and cyclic voltammetry in aqueous media. A Langmuir type adsorption and an irreversible reduction of the adsorbed complexes on the surface of the hanging-mercury electrode was detected by CV measurements. The difference polarography studies revealed a strong pH dependence of the peak potential E_p . However, E_p was not affected by the nature of the peripheral ligands or by the overall charge of the complex. In acidic media, E_p increased linearly with 56–60 mV/pH unit whereas in alkaline solutions the increase was only 28–30 mV/pH unit (20–25 °C). These results indicated the cleavage of the μ - S_2 bridges to μ -S bridges and H_2S or HS^- , respectively. The structure of the mba complex has been characterized by X-ray diffraction analysis: space group $P2_1/c$, $Z = 4$, $a = 12.086$ (2) Å, $b = 27.099$ (3) Å, $c = 14.526$ (2) Å, and $\beta = 93.63$ (1)°. In the crystal, two $[\text{Mo}_3\text{S}_7(\text{mba})_3]^{2-}$ moieties form a dimer. The COO group of one ligand is associated with the three axial sulfur atoms of a second complex and vice versa. The average O–S distance of 2.87 Å indicated a weak binding, which is discussed in terms of an anionic binding site of the Mo_3S_7 core. The observation that only one isomer is formed (all ligands are bound with S cis to the μ_3 -S atom) is discussed as a consequence of the trans effect of the μ_3 -S atom. In aqueous solution, $[\text{Mo}_3\text{S}_7(\text{H}_2\text{dsa})_3]^{2-}$ could be deprotonated to $[\text{Mo}_3\text{S}_7(\text{dsa})_3]^{8-}$. The pK values of 3.3, 3.98, 4.89, 6.77, 7.64, and 11.7 (25 °C, 0.1 M KNO_3) indicated the presence of five noncoordinated –COOH groups and one noncoordinated –SH group. Thus, in this isomer, two ligands are bound to Mo by the two S atoms and one ligand is bound by one S and one O atom.

Introduction

The preparation of compounds containing the core $[\text{Mo}_3\text{S}(\text{S}_2)_3]^{4+}$ has been extensively investigated,² and convenient routes for the synthesis of new complexes with different ligands have been developed recently.^{3–5} Since representative series of such complexes are now readily available, the influence of the peripheral ligands on the reactivity of the cluster core can be elucidated systematically. Considering the importance of MoS clusters as electron-transfer catalysts in biological systems, the redox properties of $\text{MoS}(\text{S}_2)_3$ complexes as a function of the ligand sphere are of particular interest. In this contribution, we report about the electrochemical reduction of a variety of $\text{Mo}_3\text{S}(\text{S}_2)_3$ complexes in aqueous solution.

It should be noted that most of the $\text{Mo}_3\text{S}(\text{S}_2)_3$ complexes prepared so far are soluble in organic solvents such as CH_2Cl_2 but insoluble in water. Water solubility was achieved by the use of ligands bearing additional ionizable groups. The red $[\text{Mo}_3\text{S}(\text{S}_2)_3(\text{tir})_3]^{8-}$, $\text{H}_2\text{tir}^{2-} = (\text{HO})_2\text{C}_6\text{H}_2(\text{SO}_3^-)_2$, for instance, could be prepared starting from $[\text{Mo}_3\text{S}(\text{S}_2)_3\text{Br}_6]^{2-}$. This tironato complex was very soluble in water; however, the high charge prevented the isolation of the complex as a solid compound of well-defined composition. This problem could be avoided by the use of ligands with noncoordinating carboxylic groups for solubility enhancement. In solutions with $\text{pH} \leq 3$, these complexes were only moderately soluble in water and could be precipitated and characterized by the use of suitable cations. However, in solutions of lower acidity, an increase of the overall charge caused a dramatic improvement of the solubility. Moreover, the successive deprotonation of the noncoordinating carboxylic groups allowed us to vary the overall charge of the complexes selectively and to study the influence of this alteration on the redox properties. The ligands used in this investigation were 2-mercaptosuccinic acid (H_3msa), *meso*-2,3-dimercaptosuccinic acid (H_4dsa), 2-mercaptobenzoic acid (H_2mba), and 3,4-dihydroxybenzoic acid (H_3dba).

Experimental Section

Spectroscopy and Mass Spectrometry. The UV–vis spectra were recorded on an Uvikon 820 spectrophotometer; the ^1H and ^{13}C NMR spectra were obtained by using Bruker AC-200 and Bruker WM-250 spectrometers, with a δ (ppm) scale and TMS (=0 ppm) as an internal standard. The FAB-MS spectra were run on a VG ZAB-VSEQ instru-

ment, and magnetic susceptibility was measured on a magnetic susceptibility balance (Johnson Matthey) at room temperature.

Electrochemical Measurements. The polarograms were recorded on a Metrohm E506/E608/VA 663 polarograph, using a dropping-mercury working electrode, a glassy-carbon counter electrode, and a Ag/AgCl reference.⁶ The pneumatically controlled drop time was 1 s and the scan rate 2 mV/s. In dp polarography the pulse amplitude was –50 mV.

For the cyclic voltammetry, a Metrohm 506 polarograph, a Metrohm VA E612 scanner, and a XY recorder from Phillips were used in combination with a hanging-mercury electrode and a Ag/AgCl reference.⁶ The scan rate was in the range 20–500 mV/s.

All measurements were performed in aqueous media, using sodium acetate, morpholinoethanesulfonic acid (MES), and tris(hydroxymethyl)aminomethane (Tris) for pH adjustment. Prior to CV or polarographic measurements, the solutions were deaerated by bubbling nitrogen for 5 min.

Determination of pK Values. A 50-mL volume of a test solution, containing between 0.001 and 0.002 M of the sample and 0.1 M KNO_3 , was titrated with 0.1 M KOH. A double-junction bridge configuration was used with an Ingold glass electrode, a calomel reference (0.01 M KCl, 0.09 KNO_3), and 0.1 M KNO_3 as the electrolyte. Potential measurements were performed in a waterjacketed beaker at 25.0 °C and under an atmosphere of nitrogen (washed previously with 0.1 M KNO_3). The potential was recorded on an Orion SA 720 pH meter. The electrode was calibrated by titration of 50 mL of 0.001 M HNO_3 in 0.1 M KNO_3 prior to a pK determination. The number of data points ranged between 15 and 20 per pK unit. For the determination of pK values > 7, $(\text{HNET}_3)_4[\text{Mo}_3\text{S}_7(\text{H}_2\text{dsa})(\text{Hdsa})_2]$ was converted into the potassium salt by ion exchange on Dowex 50 resin. Additional HNO_3 was added for the determination of the two lowest values. All pK's were obtained by computer evaluation. No significant deviation was found, using the two different methods given by Martell and Anderegg.⁷

- (1) (a) ETH Zürich. (b) Ciba Geigy AG, Basel, Switzerland.
- (2) (a) Müller, A.; Bhattacharyya, R. G.; Pfefferkorn, B. *Chem. Ber.* **1979**, *112*, 778. (b) Keck, H.; Kuchen, W.; Mathow, J.; Meyer, B.; Mootz, D.; Wunderlich, H. *Angew. Chem.* **1981**, *93*, 1019.
- (3) Fedin, V. P.; Sokoiov, M. N.; Mironov, Y. V.; Kolesov, B. A.; Tkachev, S. V.; Fedorov, V. Y. *Inorg. Chim. Acta* **1990**, *167*, 39.
- (4) Hegetschweiler, K.; Keller, T.; Zimmermann, H.; Schneider, W.; Schmalte, H.; Dubler, E. *Inorg. Chim. Acta* **1990**, *169*, 235.
- (5) Zimmermann, H.; Hegetschweiler, K.; Keller, T.; Gramlich, V.; Schmalte, H. W.; Petter, W.; Schneider, W. *Inorg. Chem.*, preceding paper in this issue.
- (6) 3 M KCl, $E^\circ = 0.207$ V (25 °C, 1.0 atm).
- (7) (a) Anderegg, G. *Helv. Chem. Acta* **1961**, *44*, 1673. (b) Martell, A. E.; Motekaitis, R. J. *Determination and Use of Stability Constants*; VCH: Weinheim, BRD, 1988.

* To whom correspondence should be addressed.

Table I. Crystallographic Data for $(\text{HNEt}_3)_2[\text{Mo}_3\text{S}(\text{S}_2)_3(\text{mba})_3]$

chem formula	$\text{C}_{33}\text{H}_{44}\text{N}_2\text{O}_6\text{S}_{10}\text{Mo}_3$	$V, \text{\AA}^3$	4748 (2)
fw	1173.188	Z	4
cryst size, mm	$0.35 \times 0.40 \times 0.45$	$d_{\text{calc}}, \text{g/cm}^3$	1.641
space group	$P2_1/c$ (No. 14)	$\mu(\text{Mo K}\alpha), \text{cm}^{-1}$	12.40
$a, \text{\AA}$	12.086 (2)	temp, $^\circ\text{C}$	21 $^\circ\text{C}$
$b, \text{\AA}$	27.099 (3)	R^a	0.057
$c, \text{\AA}$	14.526 (2)	R_w^b	0.069
β , deg	93.63 (1)		

$$^a R = \sum ||F_o| - |F_c|| / \sum |F_o|. \quad ^b R_w = [\sum w(|F_o| - |F_c|)^2 / \sum w|F_o|^2]^{1/2}; w = 1/\sigma^2(|F_o|).$$

Analyses. Mo was determined photometrically as bis(tironato)molybdenum(VI) (390 nm) after digestion of the sample by aqua regia. C, H, and N analyses were performed by D. Manser, Laboratorium für Organische Chemie, ETH, Zürich, Switzerland.

Materials. $(\text{NEt}_4)_2[\text{Mo}_3\text{S}_7\text{Br}_6]$ and the $[\text{Mo}_3\text{S}_7(\text{Hmsa})_3]^{2-}$ complexes were prepared as described in ref 4. Dihydroxybenzoic acid (Fluka purum) was recrystallized three times from H_2O . Octahydrohexamethylbenzotripyrrolium tribromide, $(\text{ohb})\text{Br}_3$, was prepared according to ref 8. All other reagents were commercially available products of reagent grade quality.

Preparation of $(\text{HNEt}_3)_2[\text{Mo}_3\text{S}_7(\text{mba})_3]$. A 0.50-g sample of $(\text{NEt}_4)_2[\text{Mo}_3\text{S}_7\text{Br}_6]$ was suspended in 40 mL of acetonitrile and heated to 70 $^\circ\text{C}$. A 0.40-g sample of solid H_2mba was added, and a clear solution was obtained. Triethylamine (0.8 g in 10 mL of acetonitrile) was added slowly. During the addition, a color change to red was observed and a solid precipitated. The suspension was allowed to stay at 70 $^\circ\text{C}$ for an additional 1 h and cooled to room temperature. The red solid was filtered out and dissolved in CH_2Cl_2 , and the solution was then layered with hexane/THF. The red crystals obtained (0.4 g, 82%) were suitable for X-ray structure analysis. UV/vis: $\lambda_{\text{max}} = 348 \text{ nm}$, $\epsilon = 14120$. ^{13}C NMR (CD_2Cl_2): 173.2, 146.7, 133.2, 132.8, 132.4, 123.0, 46.5, 9.1. ^1H NMR (CD_2Cl_2): 12.0 (2 H, br), 7.88 (3 H, dd, $J_1 = 7.5 \text{ Hz}$, $J_2 = 1.5 \text{ Hz}$), 7.49 (3 H, dd, $J_1 = 7.5 \text{ Hz}$, $J_2 = 1.5 \text{ Hz}$), 7.11 (3 H, td, $J_1 = 7.5 \text{ Hz}$, $J_2 = 1.5 \text{ Hz}$), 6.93 (3 H, td, $J_1 = 7.5 \text{ Hz}$, $J_2 = 1.5 \text{ Hz}$), 3.13 (12 H, q, $J = 7.3 \text{ Hz}$), 1.29 (18 H, t, $J = 7.3 \text{ Hz}$). Anal. Calc for $\text{C}_{33}\text{H}_{44}\text{N}_2\text{O}_6\text{S}_{10}\text{Mo}_3$: C, 33.79; H, 3.78; N, 2.39; Mo, 24.53. Found: C, 33.79; H, 3.79; N, 2.27; Mo, 24.25.

Preparation of Compounds Containing $[\text{Mo}_3\text{S}_7(\text{Hdba})_3]^{2-}$. A 0.75-g amount of $(\text{NEt}_4)_2[\text{Mo}_3\text{S}_7\text{Br}_6]$ was dissolved in DMF (35 mL, 100 $^\circ\text{C}$), and 1.54 g of solid H_3dba was added. The solution was stirred for 15 min at 100 $^\circ\text{C}$ followed by the dropwise addition of triethylamine (2 g, dissolved in DMF). The resulting mixture was stirred for an additional 1 h at 100 $^\circ\text{C}$ and was then allowed to cool to room temperature. The addition of 120 mL of ether resulted in the formation of a red oil, which was separated from the reaction mixture and dissolved in 60 mL of water. After the adjustment of the pH with 0.1 M NaOH to about 7, the solution was filtered and 0.6 g of NEt_4Br , dissolved in 5 mL of H_2O , was added. The pH was lowered to 2 by addition of 0.1 M HCl, and a brown solid precipitated, which was separated from its mother liquor by centrifugation. Vis: $\lambda_{\text{max}} = 412 \text{ nm}$, $\epsilon = 18300$. FAB⁺-MS: signals of $[(\text{H})_2(\text{Mo}_3\text{S}_7(\text{Hdba})_3)]^+$, $[(\text{H})_2(\text{NEt}_4)(\text{Mo}_3\text{S}_7(\text{Hdba})_3)]^+$, $[(\text{H})(\text{NEt}_4)_2(\text{Mo}_3\text{S}_7(\text{Hdba})_3)]^+$, $[(\text{NEt}_4)_3(\text{Mo}_3\text{S}_7(\text{Hdba})_3)]^+$, and $[(\text{NEt}_4)_4(\text{Mo}_3\text{S}_7(\text{Hdba})_2(\text{dba}))]^+$ (among others). For the preparation of the octahydrohexamethylbenzotripyrrolium (ohb) derivative $[\text{C}_{18}\text{H}_{30}\text{N}_3]^{2-}[\text{Mo}_3\text{S}_7(\text{Hdba})_3]^{2-} \cdot 12\text{H}_2\text{O}$, the solid was dissolved again in water and was precipitated by the addition of $(\text{ohb})\text{Br}_3$. Anal. Calc: C, 32.15; H, 3.27; N, 2.27; Mo, 23.34. Found: C, 32.38; H, 3.16; N, 2.77; Mo, 23.25.

Preparation of $(\text{HNEt}_3)_4[\text{Mo}_3\text{S}_7(\text{Hdsa})_2(\text{H}_2\text{dsa})]$. The reaction was carried out as mentioned above for the mba complex, using $(\text{NEt}_4)_2[\text{Mo}_3\text{S}_7\text{Br}_6]$ (0.75 g in 75 mL of acetonitrile), solid H_2dsa (1.82 g), and triethylamine (1.5 g in 15 mL of acetonitrile). However, after the addition of the ligand, a suspension was obtained, which was allowed to stay at 70 $^\circ\text{C}$ for 5 min before the triethylamine was added. After cooling of the mixture to room temperature, the dark brown solid was filtered out, washed with ether, and dried in vacuo. Yield: 0.45 g (34.3%). Anal. Calc for $\text{C}_{36}\text{H}_{74}\text{N}_4\text{O}_{12}\text{S}_{13}\text{Mo}_3$: C, 29.62; H, 5.11; N, 3.84; Mo, 19.72. Found: C, 29.41; H, 5.06; N, 4.15; Mo, 19.54. Vis: 339 nm (sh, $\epsilon = 11440$). FAB⁺-MS: signals of $[(\text{H})_2(\text{HNEt}_3)(\text{Mo}_3\text{S}_7(\text{H}_2\text{dsa})_3)]^+$, $[(\text{H})(\text{HNEt}_3)_2(\text{Mo}_3\text{S}_7(\text{H}_2\text{dsa})_3)]^+$, and $[(\text{HNEt}_3)_3(\text{Mo}_3\text{S}_7(\text{H}_2\text{dsa})_3)]^+$ (among others). The ohb salt $[\text{C}_{18}\text{H}_{30}\text{N}_3][\text{Mo}_3\text{S}_7(\text{H}_2\text{dsa})_3]\text{Br}$ was precipitated by the addition of $(\text{ohb})\text{Br}_3$ to a dilute aqueous solution of the obtained HNEt_3 salt. Anal. Calc: C, 25.35; H, 2.98; N, 2.96; Mo, 20.25. Found: C, 24.94; H, 2.94; N, 3.19; Mo, 20.99.

Table II. Atomic Coordinates and Isotropic or Equivalent Isotropic Displacement Parameters with Estimated Standard Deviations in Parentheses for Non-Hydrogen Atoms of $(\text{HNEt}_3)_2[\text{Mo}_3\text{S}(\text{S}_2)_3(\text{mba})_3]$

atom	x	y	z	$B, \text{\AA}^2$
Mo(1)	0.8818 (2)	0.0397 (1)	0.7098 (1)	5.26 (5)
Mo(2)	0.7997 (2)	0.0293 (1)	0.8805 (1)	5.31 (5)
Mo(3)	0.7678 (2)	-0.0438 (1)	0.7496 (1)	5.26 (5)
S(4)	0.6943 (4)	0.0355 (3)	0.7402 (4)	5.3 (2)
S(5)	0.9538 (5)	-0.0429 (3)	0.6996 (4)	5.9 (2)
S(6)	0.8408 (5)	-0.0264 (3)	0.5960 (4)	6.9 (2)
S(7)	0.7934 (5)	0.1001 (3)	0.6039 (4)	6.4 (2)
S(8)	0.9041 (6)	0.1033 (3)	0.8351 (5)	6.6 (2)
S(9)	0.9937 (5)	0.0407 (3)	0.8542 (4)	6.1 (2)
S(10)	0.6489 (5)	0.0835 (3)	0.9192 (4)	6.5 (2)
S(11)	0.6872 (5)	-0.0461 (4)	0.9039 (5)	7.0 (2)
S(12)	0.8535 (5)	-0.0550 (3)	0.9025 (4)	6.1 (2)
S(13)	0.5876 (5)	-0.0587 (3)	0.6685 (5)	6.9 (2)
O(14)	1.030 (1)	0.0618 (8)	0.652 (1)	7.8 (5)
O(15)	1.166 (1)	0.1096 (9)	0.619 (1)	9.3 (6)
O(16)	0.850 (1)	0.0363 (8)	1.021 (1)	7.4 (5)
O(17)	0.924 (1)	0.0668 (9)	1.144 (1)	10.0 (6)
O(18)	0.781 (1)	-0.1154 (8)	0.746 (1)	8.0 (5)
O(19)	0.763 (2)	-0.1993 (9)	0.741 (1)	9.8 (6)
N(20)	1.320 (1)	0.0592 (9)	0.716 (2)	7.6 (7)
N(21)	0.913 (2)	-0.220 (1)	0.882 (2)	9.4 (8)
C(22)	1.070 (2)	0.096 (1)	0.607 (1)	5.4 (6)
C(23)	0.998 (2)	0.119 (1)	0.529 (1)	5.4 (6)
C(24)	1.057 (2)	0.142 (1)	0.461 (2)	6.5 (7)
C(25)	1.004 (2)	0.167 (1)	0.387 (2)	9 (1)
C(26)	0.890 (2)	0.172 (1)	0.388 (2)	7.9 (9)
C(27)	0.832 (2)	0.148 (1)	0.452 (2)	7.0 (7)
C(28)	0.883 (2)	0.123 (1)	0.525 (2)	6.7 (7)
C(29)	0.845 (2)	0.065 (1)	1.085 (1)	5.8 (7)
C(30)	0.747 (2)	0.095 (1)	1.101 (1)	6.1 (7)
C(31)	0.736 (2)	0.114 (1)	1.189 (2)	8.4 (8)
C(32)	0.650 (2)	0.142 (1)	1.210 (2)	10 (1)
C(33)	0.562 (2)	0.149 (2)	1.143 (2)	11 (1)
C(34)	0.568 (2)	0.131 (1)	1.058 (2)	8.2 (9)
C(35)	0.659 (2)	0.104 (1)	1.033 (2)	5.7 (7)
C(36)	0.740 (2)	-0.153 (1)	0.721 (2)	6.7 (6)
C(37)	0.641 (2)	-0.158 (1)	0.638 (2)	6.0 (7)
C(38)	0.627 (3)	-0.202 (1)	0.592 (2)	11 (1)
C(39)	0.542 (3)	-0.205 (1)	0.517 (2)	12 (1)
C(40)	0.484 (2)	-0.162 (1)	0.498 (2)	10 (1)
C(41)	0.499 (2)	-0.119 (1)	0.543 (2)	7.7 (8)
C(42)	0.584 (2)	-0.115 (1)	0.619 (2)	5.9 (7)
C(43)	1.393 (3)	0.101 (1)	0.726 (2)	10 (1)
C(44)	1.355 (3)	0.137 (2)	0.791 (3)	18 (2)
C(45)	1.300 (2)	0.033 (1)	0.802 (2)	10 (1)
C(46)	1.398 (2)	0.006 (1)	0.849 (2)	10 (1)
C(47)	1.355 (2)	0.027 (1)	0.639 (2)	9.0 (9)
C(48)	1.282 (3)	-0.014 (1)	0.616 (2)	10 (1)
C(49)	1.008 (3)	-0.189 (2)	0.887 (2)	13 (1)
C(50)	1.098 (4)	-0.204 (2)	0.964 (3)	18 (2)
C(51)	0.934 (4)	-0.271 (2)	0.862 (3)	13 (1)
C(52)	0.961 (5)	-0.281 (2)	0.772 (4)	21 (2)
C(53)	0.845 (4)	-0.221 (2)	0.965 (3)	19 (2)
C(54)	0.778 (4)	-0.185 (2)	0.979 (3)	22 (2)

Table III. Summarized Bond Lengths (\AA) of the $\text{Mo}_3\text{S}_{10}\text{O}_3$ Entity in $(\text{HNEt}_3)_2[\text{Mo}_3\text{S}_7(\text{mba})_3]$ with Estimated Standard Deviations in Parentheses

bond	av value	range
Mo-Mo	2.744	2.731 (3)-2.758 (3)
Mo- μ_3 -S	2.336	2.328 (8)-2.341 (6)
Mo-S _{eq}	2.491	2.468 (8)-2.509 (8)
Mo-S _{ax}	2.410	2.393 (8)-2.423 (6)
Mo-S _{cis}	2.441	2.434 (8)-2.445 (8)
Mo-O _{trans}	2.053	1.95 (2)-2.11 (3)
S _{eq} -S _{ax}	2.021	2.017 (8)-2.026 (9)

Crystal Structure Determination and Refinement. The crystallographic data of $(\text{HNEt}_3)_2[\text{Mo}_3\text{S}(\text{S}_2)_3(\text{mba})_3]$ are summarized in Table I. The intensities of 7104 reflections were measured on a Philips PW1100 automated four-cycle diffractometer using monochromatized $\text{MoK}\alpha$ radiation. A total of 2658 reflections were classified as observed with $I > 3\sigma(I)$. The structure was solved by a combination of Patterson functions

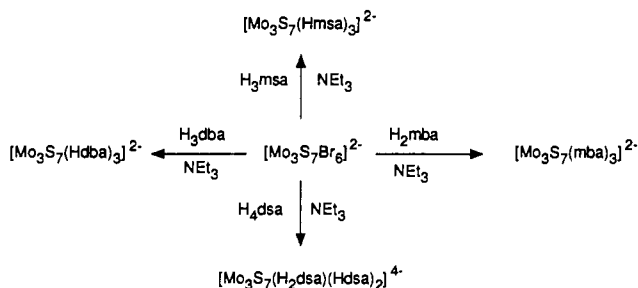
Table IV. Summarized Bond Angles (deg) of the $\text{Mo}_3\text{S}_{10}\text{O}_3$ Entity in $(\text{HNEt}_3)_2[\text{Mo}_3\text{S}_7(\text{mba})_3]$ with Estimated Standard Deviations in Parentheses

angle	av value	range
Mo-Mo-Mo	60.0	59.54 (8)-60.51 (8)
$\text{S}_{\text{ax}}-\text{Mo}-\text{O}_{\text{trans}}$	84.5	82.3 (5)-85.6 (5)
$\text{S}_{\text{ax}}-\text{Mo}-\text{S}'_{\text{ax}}$	84.1	83.1 (2)-85.7 (2)
$\text{S}_{\text{ax}}-\text{Mo}-\text{S}_{\text{cis}}$	136.3	132.7 (2)-138.3 (3)
$\text{S}_{\text{ax}}-\text{Mo}-\text{S}_{\text{eq}}$	48.7	48.4 (3)-49.0 (2)
$\text{S}_{\text{ax}}-\text{Mo}-\text{S}'_{\text{eq}}$	132.5	131.3 (2)-134.1 (2)
$\text{S}_{\text{cis}}-\text{Mo}-\text{O}_{\text{trans}}$	84.3	84.1-84.6 (5)
$\text{S}_{\text{eq}}-\text{Mo}-\text{O}_{\text{trans}}$	94.0	92.0 (5)-97.6 (5)
$\text{S}_{\text{eq}}-\text{Mo}-\text{S}_{\text{cis}}$	90.3	87.4 (2)-92.4 (2)
$\text{S}_{\text{eq}}-\text{Mo}-\text{S}'_{\text{eq}}$	172.0	170.3 (3)-173.2 (2)
$\mu_3-\text{S}-\text{Mo}-\text{O}_{\text{trans}}$	161.4	160.8 (5)-162.0 (5)
$\mu_3-\text{S}-\text{Mo}-\text{S}_{\text{ax}}$	108.9	108.1 (2)-109.4 (3)
$\mu_3-\text{S}-\text{Mo}-\text{S}_{\text{cis}}$	77.4	76.2 (2)-78.4 (2)
$\mu_3-\text{S}-\text{Mo}-\text{S}_{\text{eq}}$	86.2	84.6 (2)-88.2 (2)
$\text{Mo}-\text{S}_{\text{ax}}-\text{Mo}$	69.4	69.0 (2)-70.1 (3)
$\text{Mo}-\text{S}_{\text{ax}}-\text{S}_{\text{eq}}$	67.8	67.1 (3)-68.1 (3)
$\text{Mo}-\text{S}_{\text{eq}}-\text{Mo}$	66.9	66.7 (2)-67.1 (2)
$\text{Mo}-\text{S}_{\text{eq}}-\text{S}_{\text{ax}}$	63.6	63.0 (4)-64.1 (2)
$\text{Mo}-\mu_3-\text{S}-\text{Mo}$	72.0	71.7 (2)-72.4 (2)

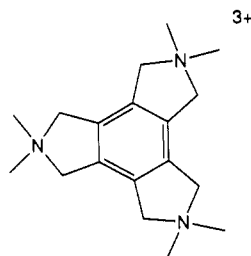
and Fourier techniques and refined by full-matrix least-squares methods with anisotropic thermal parameters for the non-hydrogen atoms. The hydrogen atoms were calculated at idealized positions and included with fixed parameters in the structure factor calculation with an isotropic thermal parameter B of 5.00 \AA^2 . Calculations were performed on a DEC Micro VAX II computer using the SDP program system.⁹ The final atomic parameters are listed in Table II, and summarized bond lengths and bond angles of the $\text{Mo}_3\text{S}_{10}\text{O}_3$ moiety are given in Tables III and IV.

Results and Discussion

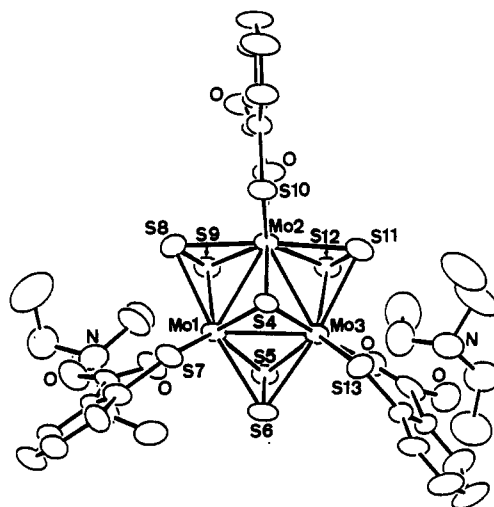
Preparation of $[\text{Mo}_3\text{S}(\text{S}_2)_3]$ Complexes. A summary of the synthetic procedure is given in the scheme



The preparation of the complexes containing mba and msa has already been published elsewhere.⁴ The dsa and the dba complexes were obtained by the same method, i.e. by simple ligand substitution from $[\text{Mo}_3\text{S}(\text{S}_2)_3\text{Br}_6]^{2-}$. As observed previously for the msa complex, the isolation and characterization of pure solids caused several difficulties. In the case of the dba complex, the excess of H_3dba , required for complete substitution, could not be separated from the complex by recrystallization or chromatographic methods (gel filtration or ion exchange). However, a compound with satisfactory elemental analysis was obtained by the precipitation of the complex with the tripositive octahydrohexamethylbenzotripyrrolium cation (ohb)



from a dilute aqueous solution. This cation had already been used

**Figure 1.** ORTEP drawing of $(\text{HNEt}_3)_2[\text{Mo}_3\text{S}(\text{S}_2)_3(\text{mba})_3]$ with numbering scheme and vibrational ellipsoids at the 20% probability level.

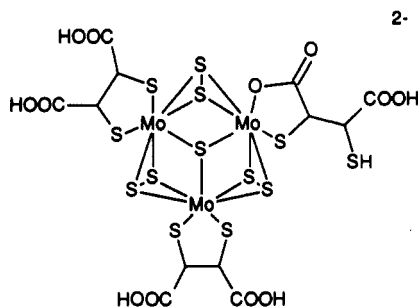
for the characterization of the mba and msa complexes. The formation of the corresponding compounds with dba and dsa confirmed the ability of ohb to precipitate anionic $\text{Mo}_3\text{S}(\text{S}_2)_3$ complexes from aqueous media as compounds of well-defined composition.

Characterization. As already reported for the msa and mba complexes, the dba and dsa complexes were obtained as diamagnetic, microcrystalline solids. The brown color of the dba complex originates from a LMCT transition at 412 nm comparable to the analogous complex with the unsubstituted catecholate ($\lambda_{\text{max}} = 424 \text{ nm}$).⁵ The spectrum of the dsa complex resembled the one of the msa and mba complex showing no maximum above 350 nm. The trinuclear structure and the composition of the four complexes have been determined unambiguously by FAB mass spectrometry. A series of signals has each been assigned to ions of the type $[(\text{H})_z(\text{X})_{3-z}(\text{Mo}_3\text{S}_7\text{L}_3)]^+$, $0 \leq z \leq 3$, $\text{X} = \text{HNEt}_3, \text{NEt}_4$, on the basis of the analysis of the isotope pattern as discussed in ref 10.

For asymmetric bidentate ligands, cis-trans isomerism is possible with respect to the location of the $\mu_3-\text{S}$ atom, and the formation of different isomers should be readily recognized by ^1H and ^{13}C NMR spectroscopy. As noted previously, the coordination of bidentate ligands with C_{2v} symmetry to the $\text{Mo}_3\text{S}(\text{S}_2)_3$ core was accompanied by a significant splitting of the peaks for the now diastereotopic parts of the ligand molecules.⁵ Thus, it can be expected that the difference of the chemical shifts is generally large enough to detect individual isomers. Actually, only one isomer was found for the mba complex which was identified by X-ray analysis as the all-cis complex (Figure 1). The ^{13}C NMR spectrum of the dsa complex showed a strong pH dependence for some of the signals and could not be completely rationalized, which indicates more than one type of ligand coordination. It was not possible to differentiate by NMR data between one isomer with differently bound ligands on the one hand and a diversity of different isomers on the other hand. However, the titration of $[\text{Mo}_3\text{S}(\text{S}_2)_3(\text{H}_2\text{dsa})_3]^{2-}$ with KOH showed three distinct buffer regions in accordance with the subsequent loss of three, two, and finally one single proton, respectively (Figure 2). The evaluation of the titration curve was in agreement with six pK values 3.3, 3.98, 4.89, 6.77, 7.64, and 11.7 (25 °C, 0.1 M KNO_3) of one single species H_6X . Close examination of the evaluated pK values suggested a structure in which two of the dsa entities are bound exclusively by $-\text{S}^-$ whereas the third dsa ligand is bound by $-\text{S}^-$ and $-\text{COO}^-$:

(9) Frenz, B. A. Enraf-Nonius SDP-Plus Structure Determination Package. Version 3.0. Enraf-Nonius, Delft, The Netherlands, 1985.

(10) Hegetschweiler, K.; Keller, T.; Amrein, W.; Schneider, W. *Inorg. Chem.* 1991, 30, 873.



The three lower pK values in the range 3.3–4.9 indicate a first deprotonation of one carboxylic acid per ligand. The deprotonation of the second carboxylic acid is observed for the two S-bounded ligands in the range pH 6–8. The last pK of 11.7 is much too high for a carboxylic acid and must be interpreted as the deprotonation of a noncoordinating $-\text{SH}$ group, as also seen for the free ligand H_4dsa (pK : 2.3, 3.5, 9.6, and 11.8).

Structure of $(\text{HNET}_3)_2[\text{Mo}_3\text{S}_7(\text{mba})_3]$. The structure of the Mo_3S_7 core is very similar to those of other complexes of this core.^{4,5,11} The three Mo atoms form an approximately equilateral triangle with an average Mo–Mo distance of 2.744 Å. This triangle is capped by the $\mu_3\text{-S}$ atom, and all Mo–Mo bonds are bridged by three disulfido groups. As a consequence of the asymmetric binding to Mo, each S_2 entity consists of an equatorial and an axial sulfur atom. The equatorial position lies approximately in the plane defined by the three Mo atoms, and the axial position is located on the opposite side of $\mu_3\text{-S}$. The three ligands are oriented approximately perpendicular to the Mo_3 plane with $-\text{S}$ in the cis and $-\text{COO}$ in the trans positions with respect to $\mu_3\text{-S}$. An ORTEP plot of the entire complex is given in Figure 1.

In the crystal structure, the $(\text{HNET}_3)_2[\text{Mo}_3\text{S}(\text{S}_2)_3(\text{mba})_3]$ entities are arranged in pairs. The COO group of one molecule is associated with the three axial S atoms of a second complex and vice versa. The average O–S distances of 2.87 Å indicate weak binding. The two other COO groups are associated with the HNET_3^+ cations by hydrogen bonding (Figure 1). It has recently been detected that the three axial sulfur atoms of the $\text{Mo}_3\text{S}(\text{S}_2)_3$ moiety form an anionic binding site.⁵ Thus, the formation of the associate $(\text{HNET}_3)_4[\text{Mo}_3\text{S}(\text{S}_2)_3(\text{mba})_3]_2$ can be interpreted as the coordination of a COO^- group to this site (Figure 3).

Electrochemical Studies. The electron uptake of the $\text{Mo}_3\text{S}(\text{S}_2)_3$ complexes in aqueous solution has been investigated by cyclic voltammetry. For all complexes, a single reduction wave has been detected in the range of -0.2 to -0.9 V vs the Ag/AgCl reference (Figure 4). The much smaller oxidation wave demonstrated unambiguously an irreversible process, and a linear dependence of the current i_p on the sweep rate v indicates adsorption of the complex on the electrode surface prior to the reduction (Figure 5). According to the theory of irreversible surface reactions,¹² the reduction peak had a characteristic asymmetric shape, with a rapid decrease of i_p to a level approximately equal to that before the reduction. This shape is a consequence of the negligible amount of molecules that are brought to the electrode by diffusion during the potential sweep compared to the amount adsorbed. At midheight, the peak width δ was found to be 30 mV regardless of the applied sweep rate v , leading to a value for $\alpha n_\alpha = 0.5$. If we consider that the symmetry factor α usually falls in the range of 0.5,¹³ one electron is transferred in the rate-limiting step.

In the difference polarogram (Figure 6) a linear dependence of the peak current upon complex concentration was found for all four compounds (Figure 7). Obviously the rather low con-

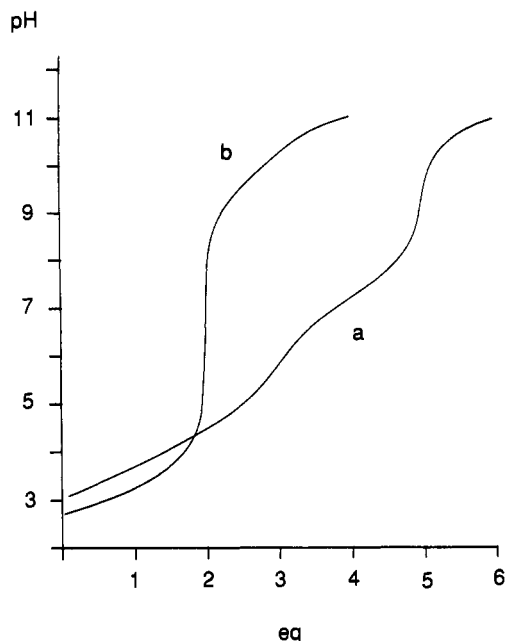


Figure 2. Neutralization of (a) $[\text{Mo}_3\text{S}_7(\text{H}_4\text{dsa})_3]^{2-}$ and (b) H_4dsa with 0.1 M KOH in 0.1 M MNO_3 (25 °C). Eq = mol KOH/mol total $[\text{Mo}_3\text{S}_7(\text{H}_4\text{dsa})_3]$ or mol KOH/mol total H_4dsa , respectively.

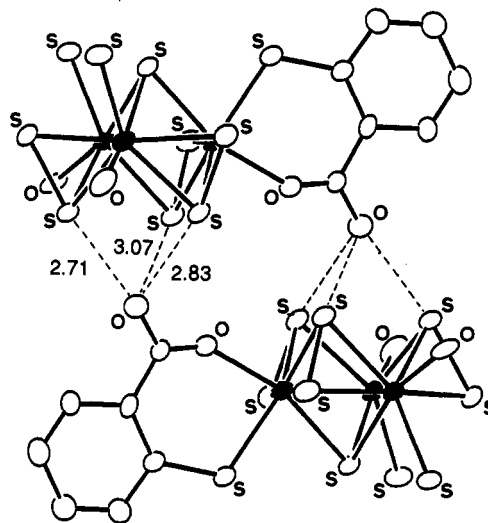


Figure 3. Anionic binding site of $[\text{Mo}_3\text{S}(\text{S}_2)_3(\text{mba})_3]^{2-}$ with S–O distances (Å) as indicated. The noncoordinating parts of two of the three ligands are omitted for clarity.

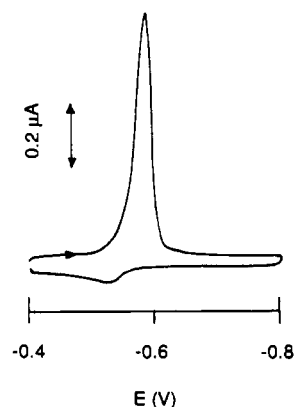


Figure 4. Cyclic voltammogram for $[\text{Mo}_3\text{S}(\text{S}_2)_3(\text{Hmsa})_3]^{2-}$. The potential of the hanging Hg electrode vs the Ag/AgCl reference is used at pH 7, scan rate 100 mV/s, and 5 μM complex solution.

centrations as used in this investigation resulted in a low coverage on the electrode surface and, consequently, in a linear dependence

- (11) (a) Marcoll, J.; Rabenau, A.; Mootz, D.; Wunderlich, H. *Rev. Chim. Miner.* 1974, 11, 607. (b) Müller, A.; Pohl, S.; Dartmann, M.; Cohen, J. P.; Benett, J. M.; Kirchner, R. M. *Z. Naturforsch.* 1979, 34B, 434. (c) Meyer, B.; Wunderlich, H. *Z. Naturforsch.* 1982, 37B, 1437. (d) Maoyu, S.; Jinling, H.; Jiayi, L. *Acta Crystallogr.* 1984, C40, 759. (e) Klingelhöfer, P.; Müller, U.; Friebel, C.; Pebler, J. *Z. Anorg. Allg. Chem.* 1986, 543, 22.
- (12) Laviron, E. *J. Electroanal. Chem. Interfacial Electrochem.* 1974, 52, 355.
- (13) Bockris, J. O'M.; Gochev, A. *J. Phys. Chem.* 1986, 90, 5232.

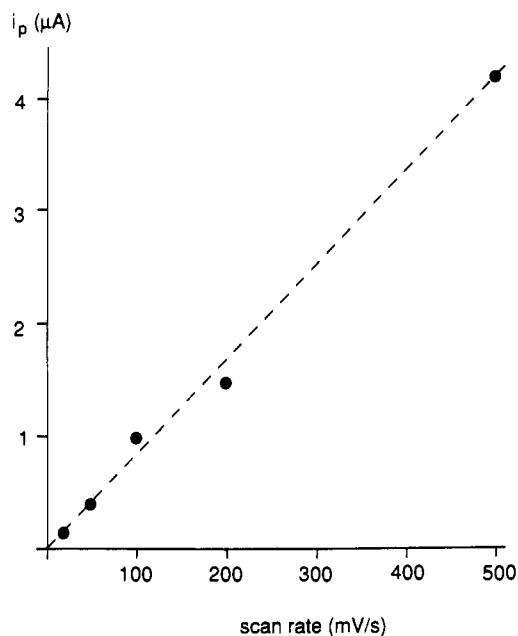


Figure 5. Cyclic voltammetry, plotting maximum peak current of the reduction wave vs scan rate ν for $[\text{Mo}_3\text{S}(\text{S}_2)(\text{Hmsa})_3]^{2-}$ at pH 7 and $5 \mu\text{M}$ complex solution.

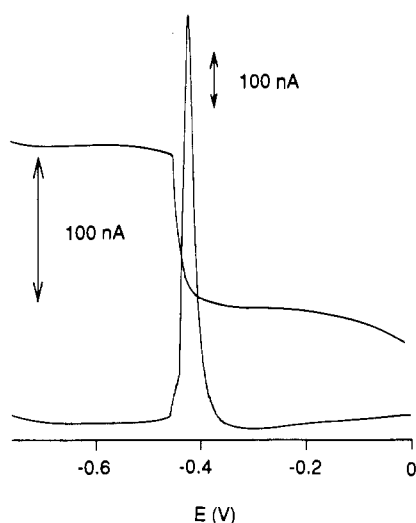


Figure 6. DC polarogram and difference polarogram for $10 \mu\text{M}$ $[\text{Mo}_3\text{S}(\text{S}_2)_3(\text{Hmsa})_3]^{2-}$ at pH 5.

Table V. Peak Potential (V) in the Difference Polarogram as a Function of Different Ligands and Variable pH (Ag/AgCl Reference; $5 \mu\text{M}$ Complex Solutions)

ligand	pH 3	pH 5	pH 7	pH 9
H ₃ msa	-0.31	-0.42	-0.52	-0.57
H ₄ dsa	-0.30	-0.41	-0.51	-0.57
H ₃ dba	-0.30	-0.41	-0.51	-0.57
H ₂ mba	-0.30	-0.42	-0.50	-0.57

of the surface concentration Γ upon the bulk concentration. The observed peak potential showed a strong pH dependence; however, no influence of the ligands or the overall charge was detected (Table V). It should be noted that the overall charge of the mba complex was not affected by the alteration of pH, but the charge of the dsa complex varied from -2 (pH 3) to -8 (pH 12) (Figure 8). The pH dependence, which has been found identical for all complexes, is presented in Figure 9: In acidic solutions (pH < 7), the peak potential decreased linearly with $56\text{--}60 \text{ mV/pH}$ unit whereas in alkaline solutions (pH > 7) a decrease of $28\text{--}30 \text{ mV/pH}$ unit was observed ($20\text{--}25 \text{ }^\circ\text{C}$). Neither the pH dependence nor the negligible influence of the ligand sphere and the overall charge are compatible with a reduction of Mo(IV). Considering an

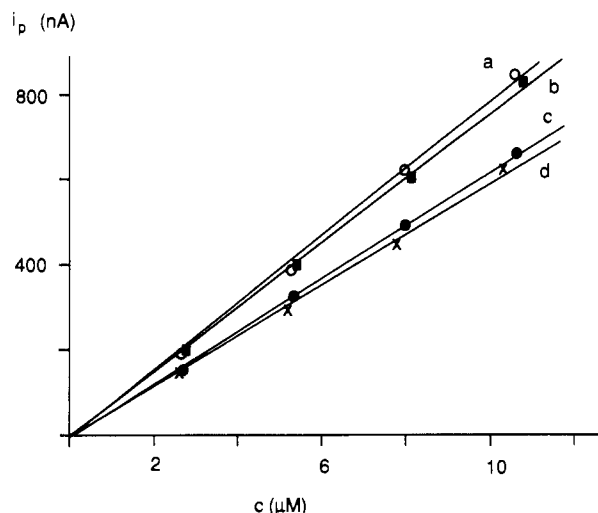


Figure 7. Maximum peak current vs concentration of the complex in the difference polarogram for (a) $[\text{Mo}_3\text{S}_7(\text{mba})_3]^{2-}$, (b) $[\text{Mo}_3\text{S}_7(\text{Hmsa})_3]^{2-}$, (c) $[\text{Mo}_3\text{S}_7(\text{Hdba})_3]^{2-}$, and (d) $[\text{Mo}_3\text{S}_7(\text{Hdsa})_2(\text{H}_2\text{dsa})]^{4-}$ at pH 5.

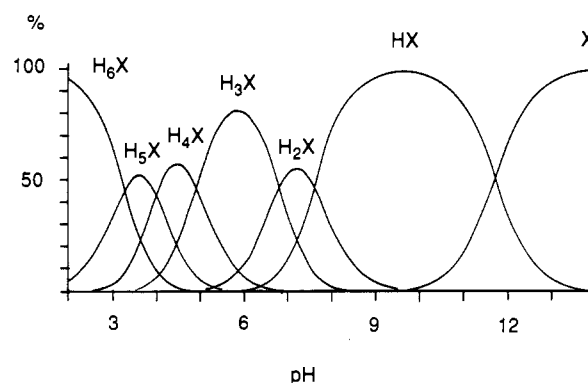


Figure 8. Equilibrium distribution of species H_nX , $\text{X} = [\text{Mo}_3\text{S}_7(\text{dsa})_3]^{8-}$.

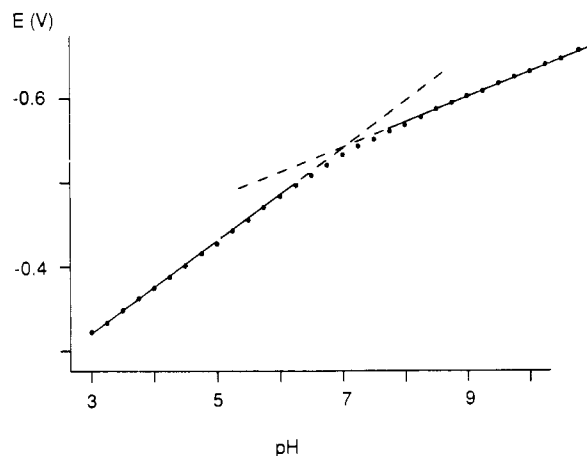
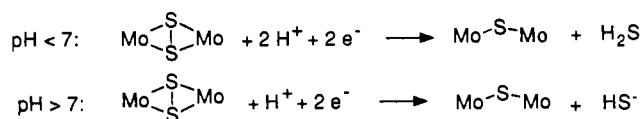


Figure 9. pH dependence of the peak potential in the difference polarogram for $[\text{Mo}_3\text{S}_7(\text{Hmsa})_3]^{2-}$, $[\text{Mo}_3\text{S}_7(\text{Hdba})_3]^{2-}$, $[\text{Mo}_3\text{S}_7(\text{mba})_3]^{2-}$, and $[\text{Mo}_3\text{S}_7(\text{H}_2\text{dsa})_3]^{2-}$ with $10 \mu\text{M}$ complex solutions and a Ag/AgCl reference.

uptake ratio of $\text{H}^+/\text{e}^- = 1$ for pH < 7 and $\text{H}^+/\text{e}^- = 0.5$ for pH > 7, the formation of H_2S or HS^- , respectively, must be taken into account (pK of $\text{H}_2\text{S} = 7$). All these results are in agreement with a two-step mechanism: (i) Langmuir-type adsorption of the complex on the electrode surface; (ii) reductive cleavage of the disulfido bridges according to the equations



Conclusions

Since asymmetric bidentate ligands are able to coordinate in two different ways to the $\text{Mo}_3\text{S}(\text{S}_2)_3$ core, the complexes with such ligands are of particular interest. The structure of the *msa* complex has been described previously.⁴ It is noteworthy that, in the *msa* as well as in the *mba* complex, the same arrangement of the ligands was found (cis position for the sulfur atoms with respect to $\mu_3\text{-S}$). Both complexes were prepared by the same procedure starting from $[\text{Mo}_3\text{S}(\text{S}_2)_3\text{Br}_6]^{2-}$. Nothing is known about the mechanistic details of the ligand substitution; however, the exclusive formation of only one type of coordination indicates a highly selective process. We believe that the high coordination number of Mo favors a dissociative substitution mechanism. The facile dissociation of Br, also observed in the gaseous phase,¹⁰ is in agreement with this assumption. A compilation of structural data about $\text{Mo}_3\text{S}(\text{S}_2)_3$ complexes with either equal monodentate ligands or bidentate C_{2v} ligands revealed clearly a significant longer Mo–ligand bond for the trans position.⁵ If we interpret this result as a trans effect of the $\mu_3\text{-S}$ atom, it seems likely that the high selectivity can be explained by the following mechanism: (i) dissociation of a Br^- in trans position; (ii) attack of a deprotonated $-\text{COO}^-$ group on Mo (with regard to this step, it is important to realize that the acidity of the SH group in acetonitrile is too low for significant deprotonation by NEt_3); (iii) substitution of the second Br^- by the mercapto group; (iv) deprotonation of the coordinated mercapto group. It has already been shown that the Mo–S bond is quite inert.⁵ Therefore, once the isomer is formed, it will keep its initial configuration.

The electrochemical studies demonstrate that in $\text{Mo}_3\text{S}(\text{S}_2)_3$ complexes the disulfido groups and not Mo(IV) were reduced on the electrode surface. This result corresponds to the reactivity of $\text{Mo}_3\text{S}(\text{S}_2)_3$ complexes with "chemical" reducing agents. As is well-known, these complexes degrade in the presence of cyanide or triphenylphosphine to Mo_3S_4 derivatives.¹⁴ In addition, it has

been shown recently that oxidizing agents attack selectively the terminal disulfido groups of $[\text{Mo}_3\text{S}(\text{S}_2)_6]^{2-}$.^{3,5} Thus, as discussed previously, the $\text{Mo}_3\text{S}(\text{S}_2)_3$ complexes are an illustrative model to show the different reactivity of coordinated disulfido groups. The stability of Mo(IV) against both reducing and oxidizing agents is quite remarkable. For *triangulo*- Mo_3S_4 complexes a reduction of Mo(IV) has been reported and complexes of the core $\text{Mo}^{\text{IV}}_2\text{-Mo}^{\text{III}}\text{S}_4$ and $\text{Mo}^{\text{IV}}\text{Mo}^{\text{III}}_2\text{S}_4$ have been postulated.¹⁵ According to the results presented in this study, the electron uptake of $\text{Mo}_3\text{S}(\text{S}_2)_3$ complexes occurs obviously by the σ^* orbital of the disulfido group and is followed by the disruption of the S–S bond. Taking into account that coordinated ligands do not affect this reactivity, reduced species with an intact $\text{Mo}_3\text{S}(\text{S}_2)_3$ core can hardly exist at all.

Acknowledgment. We thank Ruth Blumer and Dr. Heinz Rügger for the measurements of the NMR spectra, Dr. F. Behm for helpful advice, and Dr. R. Kissner and Dr. S. Wunderli for helpful discussions about the interpretation of the electrochemical measurements. The support of this work by the Swiss National Science Foundation is gratefully acknowledged.

Registry No. $(\text{HNEt}_3)_2[\text{Mo}_3\text{S}_7(\text{mba})_3]$, 129198-30-7; $(\text{NEt}_4)_2[\text{Mo}_3\text{S}_7\text{Br}_6]$, 127294-35-3; $[\text{C}_{18}\text{H}_{30}\text{N}_3]_2[\text{Mo}_3\text{S}_7(\text{Hdba})_3]$, 136061-36-4; $(\text{HNEt}_3)_4[\text{Mo}_3\text{S}_7(\text{Hdsa})_2(\text{Hzdsa})]$, 136061-34-2; $[\text{Mo}_3\text{S}_7(\text{Hmsa})_3]^{2-}$, 136172-03-7; $[\text{Mo}_3\text{S}_7(\text{msa})_3]^{2-}$, 129262-36-8; $[\text{Mo}_3\text{S}_7(\text{mba})_3]^{2-}$, 129262-31-3; $[\text{Mo}_3\text{S}_7(\text{Hdba})_3]^{2-}$, 136061-32-0; $[\text{Mo}_3\text{S}_7(\text{Hdsa})_2(\text{H}_2\text{dsa})]^{4-}$, 136061-31-9; $[\text{Mo}_3\text{S}_7(\text{H}_2\text{dsa})]^{2-}$, 136061-30-8; S, 7704-34-9; Hg, 7439-97-6.

Supplementary Material Available: Tables SI–SIV, listing crystallographic data, anisotropic displacement parameters, and bond distances and angles, and Figures S1–S3, showing the FAB⁺ mass spectra of $(\text{NEt}_4)_2[\text{Mo}_3\text{S}_7(\text{Hdba})_3]$ and $(\text{HNEt}_3)_4[\text{Mo}_3\text{S}_7(\text{H}_2\text{dsa})(\text{Hdsa})_2]$ and a stereoview of the unit cell of $(\text{HNEt}_3)_2[\text{Mo}_3\text{S}_7(\text{mba})_3]$, respectively (10 pages); a table of calculated and observed structure factors (12 pages). Ordering information is given on any current masthead page.

(14) (a) Müller, A.; Reinsch, U. *Angew. Chem.* **1980**, *92*, 69. (b) Keck, H.; Kuchen, W.; Mathow, J.; Wunderlich, H. *Angew. Chem.* **1982**, *94*, 927. (c) Halbert, T. R.; McGauley, K.; Pan, W.-H.; Czernuszewicz, R. S.; Stiefel, E. I. *J. Am. Chem. Soc.* **1984**, *106*, 1849.

(15) (a) Wiegardt, K.; Herrmann, W.; Müller, A.; Eltner, W.; Zimmermann, M. Z. *Naturforsch.* **1984**, *39B*, 876. (b) Shibahara, T.; Kuroya, H. *Polyhedron* **1986**, *5*, 357.

Contribution from the Dipartimento di Chimica Inorganica e Metallorganica e Centro CNR and Istituto di Chimica Strutturistica Inorganica, Università degli Studi di Milano, via G. Venzian 21, I 20133 Milano, Italy

Reaction of Dioxygen with $[\text{Cu}(\text{dmpz})_n]$ ($\text{Hdmpz} = 3,5\text{-Dimethylpyrazole}$). Crystal Structure, Reactivity, and Catalytic Properties of $[\text{Cu}_8(\text{dmpz})_8(\text{OH})_8]$

G. Attilio Ardizzoia,^{1a} M. Angela Angaroni,^{1a} Girolamo La Monica,^{*,1a} Franco Cariati,^{1a} Sergio Cenini,^{1a} Massimo Moret,^{*,1b} and Norberto Masciocchi^{1b}

Received April 23, 1991

The species $[\text{Cu}_8(\text{dmpz})_8(\text{OH})_8]$ (**2**) ($\text{Hdmpz} = 3,5\text{-dimethylpyrazole}$) has been obtained by reacting $[\text{Cu}(\text{dmpz})_n]$ (**1**) with O_2 at atmospheric pressure and room temperature in wet solvents. Crystal data for $[\text{Cu}_8(\text{dmpz})_8(\text{OH})_8] \cdot 2\text{C}_6\text{H}_5\text{NO}_2$ (22 °C): $a = 10.229$ (3) Å, $b = 27.217$ (2) Å, $c = 14.532$ (1) Å, $\beta = 98.51$ (1)° with $Z = 2$ in the space group $P2_1/m$. $[\text{Cu}_8(\text{dmpz})_8(\text{OH})_8]$ consists of a discrete octameric molecule with a cyclic planar system of copper(II) atoms, bridged by OH and *dmpz* ligands, forming a molecule of toroidal shape; in the crystal, its cavity (viable diameter of ca. 6 Å) contains crystallographically disordered, possibly water, molecules; in addition, fully ordered clathrated nitrobenzene molecules have been found between the octameric units. Complex **2** is catalytically active in the oxidation reactions of organic substrates such as triphenylphosphine, aromatic primary amines, dibenzylamine, and carbon monoxide, triphenylphosphine oxide, azobenzenes, *N*-benzylidenebenzylamine and carbon dioxide being respectively formed. Its reaction with PPh_3 under an inert atmosphere gave 4 mol of $\text{O}=\text{PPh}_3$ per mole of **2**, suggesting that **2** gives rise, in solution, to tautomeric species of the general formula $[\text{Cu}_8(\text{dmpz})_8(\text{O})_x(\text{OH})_{8-2x}(\text{H}_2\text{O})_x]$ ($x = 1\text{--}4$), which might behave as the active species. Complex **2** allowed also the stoichiometric oxidation of cyclohexyl isocyanide into the corresponding isocyanate in the absence or in the presence of O_2 . The reaction of **2** with primary alcohols $\text{R}'\text{OH}$ ($\text{R}' = \text{Me}, \text{Et}, \text{Pr}^n$, allyl) affords the octaalkoxo derivatives $[\text{Cu}_8(\text{dmpz})_8(\text{OR}')_8]$ (**3**) whose formulation is suggested on the basis of analytical and spectroscopic data, as well as on chemical properties.

Introduction

Polynuclear complexes are of interest because of their bonding and magnetic interactions and also because of their potential role

in catalysis.² The reaction of dioxygen with copper-containing compounds occurs in a large variety of important synthetic, in-

(1) (a) Dipartimento di Chimica Inorganica e Metallorganica e Centro CNR. (b) Istituto di Chimica Strutturistica Inorganica.

(2) (a) McKee, V.; Tandon, S. S. *J. Chem. Soc., Dalton Trans.* **1991**, 221. (b) Hoskins, B. F.; Robson, R.; Smith, P. *J. Chem. Soc., Chem. Commun.* **1990**, 488.